Observation of Two-Mode Squeezing in a Traveling Wave Parametric Amplifier

Martina Esposito,[1,2,*] Arpit Ranadive,[1,*] Luca Planat,[1] Sébastien Leger,[1] Dorian Fraudet,[1] Vincent Jouanny,[1] Olivier Buisson,[1] Wiebke Guichard,[1] Cécile Naud,[1] José Aumentado,[3] Florent Lecocq,[3] and Nicolas Roch[1]

[1]*Université Grenoble Alpes, CNRS, Grenoble INP, Institut Néel, 38000 Grenoble, France*
[2]*CNR-SPIN Complesso di Monte S. Angelo, via Cintia, Napoli 80126, Italy*
[3]*National Institute of Standards and Technology, Boulder, Colorado 80305, USA*

(Received 9 November 2021; accepted 18 March 2022; published 15 April 2022)

Traveling wave parametric amplifiers (TWPAs) have recently emerged as essential tools for broadband near quantum-limited amplification. However, their use to generate microwave quantum states still misses an experimental demonstration. In this Letter, we report operation of a TWPA as a source of two-mode squeezed microwave radiation. We demonstrate broadband entanglement generation between two modes separated by up to 400 MHz by measuring logarithmic negativity between 0.27 and 0.51 and collective quadrature squeezing below the vacuum limit between 1.5 and 2.1 dB. This work opens interesting perspectives for the exploration of novel microwave photonics experiments with possible applications in quantum sensing and continuous variable quantum computing.

DOI: 10.1103/PhysRevLett.128.153603

Frequency conversion and wave-mixing processes in nonlinear media allow manipulation and control of the electromagnetic radiation [1] and are extensively used for a broad range of applications including, for example, coherent high harmonics generation [2], nonlinear spectroscopy [3], nonlinear imaging [4], and quantum optics experiments for the generation of entanglement and squeezing [5,6]. In the past two decades, it became possible to tailor such nonlinear interactions by engineering artificial media with specifically designed nonlinear properties: nonlinear metamaterials [7–9]. Superconducting quantum circuits based on Josephson junctions recently gained a key role in this framework, since they can be used to engineer strong nonlinearities without dissipation.

Josephson-junction-based nonlinear metamaterials [7,8] have been successfully implemented as near quantum-noise-limited traveling wave parametric amplifiers (TWPAs) [10–15]. However, the potential of these devices goes far beyond amplification: Since they offer large bandwidth and flexible customization of the desired nonlinear response, they have been identified as very promising for the generation of two-mode squeezing and broadband entanglement [16–18].

Two-mode squeezing in superconducting circuits has been demonstrated in narrow-band Josephson parametric amplifiers based on resonant structures [19–26], semi-infinite transmission lines via dynamical Casimir effect [27–29] and surface acoustic wave hybrid systems [30].

The use of TWPAs as entanglement and two-mode squeezing sources would have the advantage of a large instantaneous bandwidth and customizable nonlinearities, with potential novel applications for quantum sensing [31,32], quantum enhanced detection [33], quantum teleportation with propagating waves [34], and quantum information with continuous variables [35–37].

For TWPA devices, however, the presence of loss [38–40] and the activation of spurious nonlinear processes, such as harmonics [41] and sideband generation [42], have very recently been identified as strong limitations for the observation of squeezing.

In this Letter, by using an improved fabrication process [43,44] and optimizing the device length to mitigate internal loss, we demonstrate generation of vacuum two-mode squeezing in a Josephson TWPA.

The device is driven with a pump microwave tone at frequency f_p, and the generated two-mode quantum state is characterized via repeated measurements of the field quadratures at the signal and idler frequencies f_s and f_i, respectively, such that $2f_p = f_s + f_i$ (four-wave-mixing interaction). Given the broadband nature of TWPAs, entangled pairs of signal and idler photons are generated in the entire amplification bandwidth of the device. The entanglement between signal and idler modes is quantified by the reconstruction of the two-mode covariance matrix [45] and the estimation of the logarithmic negativity [46]. We obtain nonzero logarithmic negativity and inferred squeezing of the collective quadratures between 1.5 and 2.1 dB below the vacuum limit, for a maximum frequency separation between signal and idler of 400 MHz, set by the capability of the adopted experimental setup. In addition, we verify the stability in time of the entanglement generation by studying the statistical distribution of experiments repeated over a timescale of hours.

The adopted device is a Josephson TWPA whose unit cell consists in a superconducting nonlinear asymmetric inductive element (SNAIL) [47] operated in a dilution

refrigerator at 20 mK. Such a Josephson metamaterial has been recently demonstrated and successfully operated as a near quantum-limit broadband microwave amplifier [15]. The device used in this experiment is similar to the one presented in Ref. [15], with the only difference of a reduced length of the medium (250 cells) for loss mitigation (see Supplemental Material [48] for details). The device is operated in the four-wave-mixing regime at zero flux. An external magnetic flux threading the SNAIL loops is set by a superconducting coil located alongside the device sample holder to counter stray fields.

When the TWPA is driven with pump frequency f_p, photon pairs are generated at signal and idler frequencies f_s and f_i such that $f_{s/i} = f_p \pm \Delta$, via a two-mode squeezing interaction [45]. In the absence of other frequency conversion or wave-mixing processes and neglecting losses, the input two-mode (signal-idler) vacuum state is transformed at the output of the TWPA into a two-mode squeezed state: $|\mathrm{TMS}\rangle = \hat{S}|0\rangle_s|0\rangle_i$. The two-mode squeezing operator is

$$\hat{S} = \exp\left(\xi \hat{a}^\dagger_{s,\mathrm{in}} \hat{a}^\dagger_{i,\mathrm{in}} - \xi^* \hat{a}_{s,\mathrm{in}} \hat{a}_{i,\mathrm{in}}\right), \tag{1}$$

where $\xi = re^{i\phi}$ is the squeezing parameter and $\hat{a}_{s,\mathrm{in}}$ ($\hat{a}_{i,\mathrm{in}}$) is the signal (idler) mode operator at the input of the TWPA.

A sketch of the experimental setup and device is shown in Fig. 1(a). The device is driven with a pump tone, and the two-mode quantum state generated at the output undergoes an amplification chain, from 20 mK to room temperature, with total system gain G_{sys}. At room temperature, a double heterodyne detection scheme allows the detection of signal and idler fields: The output microwave radiation is analogically down-converted to an intermediate frequency, split in two paths, and digitized using a multichannel acquisition board with a sampling clock set to 2 GSamples/s (see Supplemental Material [48] for a detailed description of the setup). Digital down-conversion is then performed on board. The resolution bandwidth is defined by the inverse of the acquisition time $\tau = 6\ \mu$s.

The raw measured observables are the signal and idler field quadratures:

$$\hat{X}_{s/i} = \frac{1}{2}(\hat{A}_{s/i} + \hat{A}^\dagger_{s/i}), \qquad \hat{P}_{s/i} = \frac{1}{2i}(\hat{A}_{s/i} - \hat{A}^\dagger_{s/i}), \tag{2}$$

where $\hat{A}^\dagger_{s/i}$ and $\hat{A}_{s/i}$ are the creation and annihilation operators, respectively, for the signal and idler mode such that $[\hat{A}_j, \hat{A}^\dagger_k] = \delta_{j,k}$.

A single acquisition consists in measuring the raw quadratures with the pump both switched off and switched on. A sketch of the control-readout pulse sequence for a single on-off acquisition is shown in Fig. 1(c).

Once the raw quadrature data are measured, they are normalized by the gain of the detection chain at signal and idler frequency, respectively:

$$x_{s/i} = X_{s/i}/\sqrt{G_{\mathrm{sys},s/i}}, \qquad p_{s/i} = P_{s/i}/\sqrt{G_{\mathrm{sys},s/i}}.$$

The estimation of the system gain, $G_{\mathrm{sys},s/i}$, is obtained by using a shot noise tunnel junction noise source [53–55] (see Supplemental Material [48] for details).

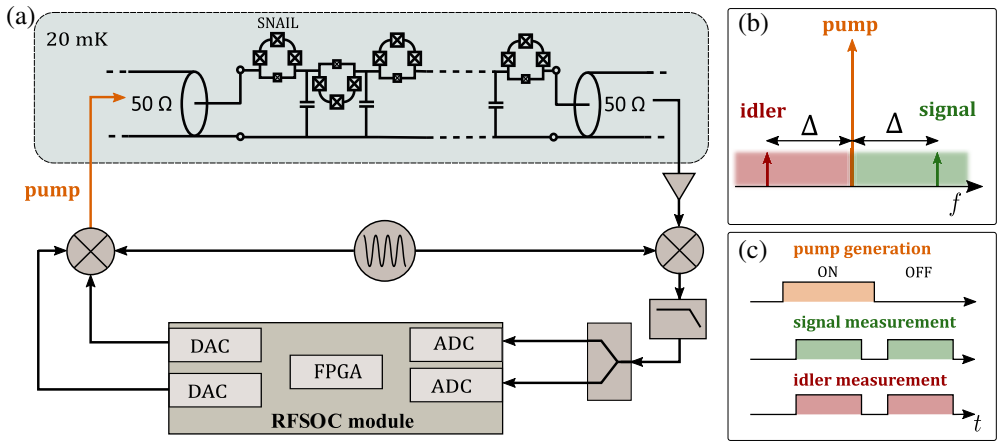

FIG. 1. (a) Simplified sketch of the experimental setup for two-mode squeezing generation and detection. The Josephson TWPA device is composed of 250 SNAIL-based unit cells, and it is anchored at the 20 mK stage of a dilution refrigerator. The input pump field is obtained via up conversion with an IQ mixer: The I and Q inputs at an intermediate frequency ($f_{\text{pump-IF}} = 290$ MHz) are mixed with a microwave local oscillator (generated with an rf source). The output microwave radiation is amplified, down-converted with a mixer, split in two paths, and finally digitized. The room temperature electronics is composed by an rf system-on-chip (RFSOC) acquisition board with an integrated field programmable gate array (FPGA), two digital to analog converters (DACs), used to generate the pulsed intermediate frequency inputs for the IQ mixer, and two analog to digital converters (ADCs), used for digitizing the down-converted output radiation. (b) Sketch of the frequency spacing between the pump and a pair of signal and idler. (c) Sketch of the control and readout pulse sequence for a single pump on-off generation and measurement; the duration of the readout pulses (acquisition time) is 6 μs.

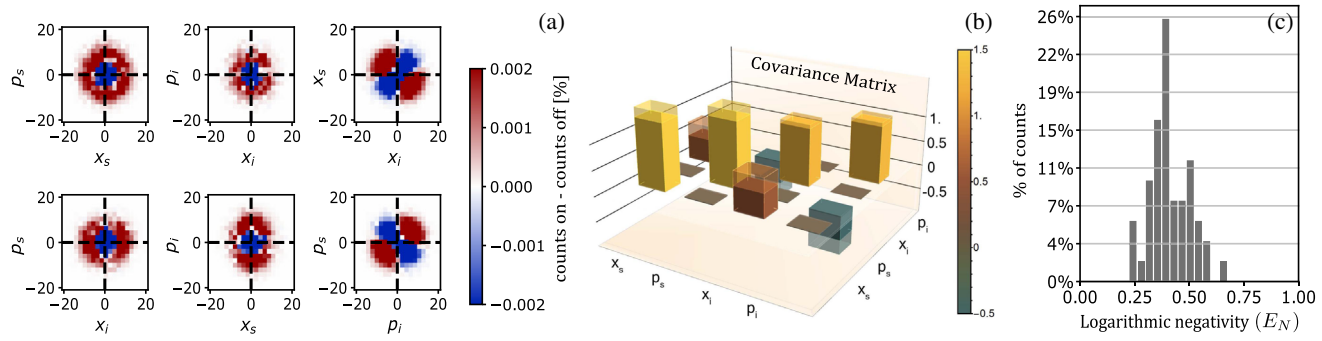

FIG. 2. (a) Measured quadrature phase space distribution (two-dimensional differential histogram plots: difference between pump on and pump off histograms) for 10^8 on-off acquisitions and detuning $\Delta = 200$ MHz; the shape of the differential quadrature distributions in the (x_i, x_s) and (p_i, p_s) phase spaces indicates the presence of two-mode correlations. (b) Reconstructed covariance matrix with uncertainty indicated by shaded regions. (c) Entanglement stability over time: histogram of 50 repeated entanglement measurements, each obtained from a set of 2×10^6 repeated on-off quadrature acquisitions. Pump frequency $f_p = 4.415$ GHz.

We stress that a careful calibration of $G_{\mathrm{sys},s/i}$ is necessary for a quantitative estimation of the amount of entanglement and squeezing. It should be noticed that here we use an upper bound estimation for G_{sys} (see Supplemental Material [48]). This choice gives a rigorous lower bound estimation for the amount of entanglement and squeezing.

The same acquisition is repeated for N_{rep} times, obtaining, for pump both off and on, six two-dimensional quadrature histograms (combinations of the four measured quadratures). For $N_{\mathrm{rep}} = 10^8$, the full on-off experiment takes about one hour.

Experimentally obtained quadrature histograms for detuning $\Delta = 200$ MHz and $N_{\mathrm{rep}} = 10^8$ are shown in Fig. 2(a). Each two-dimensional histogram is obtained by subtracting the histogram with the pump off from the histogram with the pump on.

Starting from the measured quadratures, we estimate the covariance matrix [45] of the generated bipartite quantum state. This matrix encodes all the quantum properties of the generated state. We compute the covariance matrix from the experimental data for both pump on and pump off as

$$\boldsymbol{\sigma}_{jk}^{\mathrm{meas}} = 4\left[\frac{1}{2}\langle R_j R_k + R_k R_j\rangle - \langle R_j\rangle\langle R_k\rangle\right], \tag{3}$$

where $\mathbf{R} = (x_s, p_s, x_i, p_i)$. The covariance matrix of the two-mode quantum state generated at the output of the TWPA can be inferred by subtracting the pump-off noise background as follows [21]:

$$\boldsymbol{\sigma} = \boldsymbol{\sigma}^{\mathrm{meas,on}} - \boldsymbol{\sigma}^{\mathrm{meas,off}} + \mathbb{1}_4, \tag{4}$$

where, with the adopted convention, the two-mode vacuum state covariance matrix corresponds to the unit matrix.

The inferred covariance matrix is depicted in Fig. 2(b). The presence of not vanishing off-diagonal elements indicates two-mode squeezing correlations between the signal and idler, verifying a necessary condition for the demonstration of entanglement generation.

A quantitative entanglement estimation is provided by the logarithmic negativity $E_{\mathcal{N}}$ [46] defined as $E_{\mathcal{N}} = \mathrm{Max}[-\ln(\nu_-), 0]$, where ν_- is the minimum symplectic eigenvalue of the partially transposed covariance matrix (see Supplemental Material [48]). Following the partial positive transpose criterion [56], the logarithmic negativity being positive ($E_{\mathcal{N}} > 0$) is a sufficient condition to demonstrate that the state is entangled.

For the data shown in Fig. 2, we measure a logarithmic negativity $E_{\mathcal{N}} = 0.4 \pm 0.1$, which proves entanglement generation, i.e., quantum nature of observed correlations.

The pump power is optimized to get the maximum entanglement (maximum logarithmic negativity). This is reached for a linear gain $G = 1.30 \pm 0.05$, corresponding to a squeezing parameter $r = \mathrm{arcosh}(\sqrt{G}) = 0.52 \pm 0.04$. For higher pump powers, that is, higher TWPA gain G, we observe a decrease of the logarithmic negativity (see Supplemental Material [48]). Similar behavior has been observed in resonant Josephson parametric amplifiers [57] and semi-infinite transmission lines [29], due to the activation of spurious higher-order and wave-mixing processes. In TWPAs, the role of such spurious processes on limiting the amount of generated squeezing is currently an open question. Further explorations of the high pump power regime is beyond the scope of this Letter.

The stability of the generated entanglement over time is verified by performing 50 repetitions of the same experiment (each consisting of a set of 2×10^6 quadrature acquisitions) over a total time of roughly one hour. In Fig. 2(c), we show the obtained histogram distribution of the logarithmic negativity. This result demonstrates that the generated entanglement is stable for repeated measurements over a timescale of hours.

A largely adopted second criterion to verify the nonclassicality of the generated bipartite state consists in estimating the variances of the collective quadratures:

$$\hat{x}_+ = (\hat{x}_s + \hat{x}_i), \qquad \hat{p}_+ = (\hat{p}_s + \hat{p}_i), \tag{5}$$

and compare them with the vacuum noise [19,20,38].

Considering a squeezing parameter amplitude r and accounting for average TWPA loss, $0 \leq \bar{\epsilon} \leq 1$, with a simple lumped-element beam splitter model (see Supplemental Material [48]), the variance of the collective quadrature can be expressed as [38]

$$\langle x_+^2 \rangle = \frac{1}{2}[\bar{\epsilon} + (1 - \bar{\epsilon})e^{-2r}]. \tag{6}$$

For a nonclassical state, the latter is expected to be lower than the vacuum quantum noise giving nonzero squeezing, defined as $\mathrm{Sq}_+ = 10 \log(\langle x_+^2 \rangle / 0.5)$.

For the data shown in Fig. 2, we obtain a lower bound on the squeezing value: $\mathrm{Sq}_+ = -1.6 \pm 0.5$ dB below the vacuum limit.

In the adopted pump power regime, the obtained squeezing value is limited by the effect of internal loss present in the device: For fixed TWPA gain, a device with higher loss (composed of a higher number of unit cells) will generate a reduced amount of squeezing. We designed the length of the TWPA device, 250 unit cells, to mitigate internal loss and foster the squeezing generation for a fixed gain value (see Supplemental Material [48]).

In Fig. 3, we show the pump phase dependence of the generated two-mode squeezing. By varying the pump input phase, we observe the expected periodicity of the collective quadrature variances [Fig. 3(a)] and, consequently, of the squeezing Sq_+ [Fig. 3(b)]. In Fig. 3(c), the experimentally obtained logarithmic negativity $E_\mathcal{N}$ is reported. We stress that this is a conservative lower bound estimation (an upper bound estimation for G_{sys} is considered, giving a lower bound estimation of the amount of entanglement). The gray shadowed area indicates the logarithmic negativity predicted by a simple two-mode squeezing model that considers the measured TWPA gain and estimated device losses (see Supplemental Material [48] for details).

A key advantage in generating two-mode squeezing with TWPAs is their broadband nature: When the pump drives the device, all the pairs of signal and idler modes within the TWPA bandwidth (several gigahertz [17]) get entangled. To quantify the broadband nature of the generated entangled states, we estimate the rate of entangled bit generation by calculating the entropy formation $E_F = c_+ \log_2 c_+ - c_- \log_2 c_-$, with $c_\pm = (\delta^{-1/2} \pm \delta^{1/2})^2/4$ and $\delta = 2^{E_\mathcal{N}}$ [20,58], and multiplying it by the squeezing bandwidth 2Δ. Despite the fact that bandwidth of our device is in the gigahertz range, we could check only entanglement between signal and idler separated by a maximum of $2\Delta = 400$ MHz because of limitations of the adopted acquisition system. We use such bandwidth to obtain a lower bound of 53 ± 20 Mebit/s (mega entangled bits per second) on the rate of entanglement generation, which is already comparable with previous state of the art (Supplemental Material in Ref. [29]).

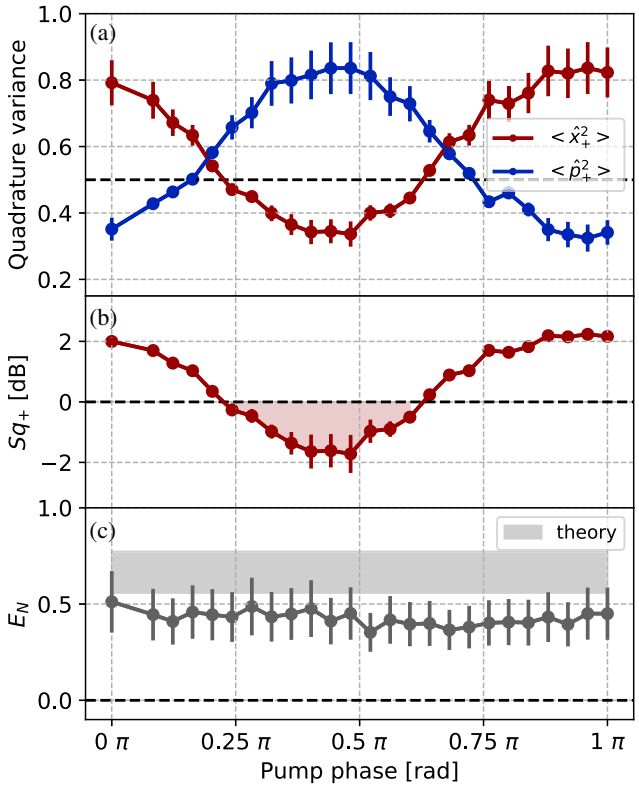

FIG. 3. Collective quadrature variance (a), squeezing (b), and logarithmic negativity (c) as a function of the input pump phase. Pump frequency $f_p = 4.415$ GHz; detuning $\Delta = 200$ MHz; number of repeated measurements for each phase $N_{\mathrm{rep}} = 10^7$. Dashed lines indicate the vacuum state reference. Squeezing below the vacuum limit is highlighted with a shadow area in (b). The gray shadow area in (c) indicates the logarithmic negativity predicted by a simple lumped-element model which takes into account the TWPA gain and the estimated losses (see Supplemental Material [48]).

Finally, to further investigate the entanglement generation within the available frequency bandwidth, we vary the detuning Δ between the pump frequency and the signal and idler frequencies. For each value of the detuning, we measure the logarithmic negativity and the squeezing. The results are shown in Fig. 4. We observe entanglement and two-mode squeezing in the entire investigated frequency region. This result further demonstrates the truly broadband nature of squeezing generation in the device under study. We again report the comparison between our lower bound estimation of the logarithmic negativity and the prediction of a simple lumped-element model which takes into account measured TWPA gain and internal loss.

In conclusion, we demonstrated two-mode squeezing generation in a traveling wave parametric amplifier. This result proves that TWPAs can be effectively used as sources of microwave radiation. We obtained broadband squeezing

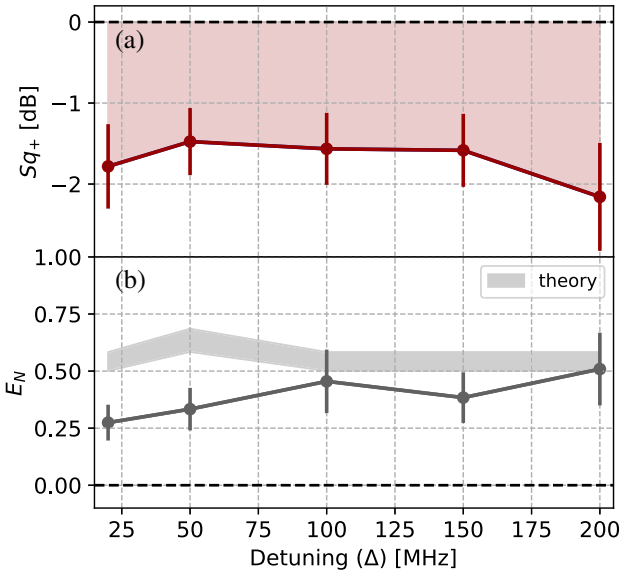

FIG. 4. Two-mode squeezing (a) and logarithmic negativity (b) as a function of detuning Δ. Pump frequency $f_p = 4.415$ GHz; number of repeated measurements for each Δ, $N_{\mathrm{rep}} = 10^7$. Dashed lines indicate the vacuum state reference. The gray shadowed area in (b) indicates the logarithmic negativity predicted by a simple lumped-element model which takes into account the TWPA gain and the estimated loss (see Supplemental Material [48]).

of between 1.5 and 2.1 dB for signal and idler modes separated by up to 400 MHz. This first result can be further improved via a deeper understanding of loss mechanisms and higher-order nonlinear effects in TWPAs. Another interesting direction will be to take advantage of flexibility offered by TWPAs to explore different wave-mixing processes and tailored nonlinearities.

On a broad prospective, our findings experimentally demonstrate the potential of TWPA devices beyond amplification, paving the way to their application in the context of microwave photonics, quantum sensing, and quantum information with continuous variables.

Certain commercial equipment, instruments, or materials are identified in this Letter in order to specify the experimental procedure adequately. Such identification is not intended to imply recommendation or endorsement, nor is it intended to imply that the materials or equipment identified are necessarily the best available for the purpose.

The data supporting the findings presented in this Letter are openly available [59].

This work is supported by the European Union's Horizon 2020 research and innovation program under Grant Agreement No. 899561. M. E. acknowledges the European Union's Horizon 2020 research and innovation program under the Marie Sklodowska Curie (Grant Agreement No. MSCA-IF-835791). A. R. acknowledges the European Union's Horizon 2020 research and innovation program under the Marie Sklodowska Curie Grant Agreement No. 754303 and the "Investissements d'avenir" (ANR-15-IDEX-02) programs of the French National Research Agency. The sample was fabricated in the clean room facility of Institute Neel, Grenoble; we sincerely thank all the clean room staff for help with fabrication of the devices. We acknowledge E. Eyraud for his extensive help in the installation and maintenance of the cryogenic setup and J. Minet for significant help in programming the high-speed pulse generation and data acquisition setup. We also thank J. Jarreau and L. Del Rey for their support with the experimental equipment. We are grateful to B. Boulanger, A. Metelmann, and S. Böhling for insightful discussions regarding this project. We thank the members of the superconducting circuits group at Neel Institute for helpful discussions. We sincerely thank M. Malnou and J. D. Teufel for their careful reading of the manuscript.

[*] These authors contributed equally to this work.

[1] R. W. Boyd, *Nonlinear Optics*, 3rd ed. (Elsevier, New York, 2008).
[2] S. Kim, J. Jin, Y. J. Kim, I. Y. Park, Y. Kim, and S. W. Kim, High-harmonic generation by resonant plasmon field enhancement, Nature (London) **453**, 757 (2008).
[3] M. Geissbuehler, L. Bonacina, V. Shcheslavskiy, N. L. Bocchio, S. Geissbuehler, M. Leutenegger, I. Märki, J. P. Wolf, and T. Lasser, Nonlinear correlation spectroscopy (NLCS), Nano Lett. **12**, 1668 (2012).
[4] M. V. DaCosta, S. Doughan, Y. Han, and U. J. Krull, Lanthanide upconversion nanoparticles and applications in bioassays and bioimaging: A review, Anal. Chim. Acta **832**, 1 (2014).
[5] S. Barz, G. Cronenberg, A. Zeilinger, and P. Walther, Heralded generation of entangled photon pairs, Nat. Photonics **4**, 553 (2010).
[6] M. A. Castellanos-Beltran, K. D. Irwin, G. C. Hilton, L. R. Vale, and K. W. Lehnert, Amplification and squeezing of quantum noise with a tunable Josephson metamaterial, Nat. Phys. **4**, 929 (2008).
[7] M. Lapine, I. V. Shadrivov, and Y. S. Kivshar, Colloquium: Nonlinear metamaterials, Rev. Mod. Phys. **86**, 1093 (2014).
[8] P. Jung, A. V. Ustinov, and S. M. Anlage, Progress in superconducting metamaterials, Supercond. Sci. Technol. **27**, 073001 (2014).
[9] A. Krasnok, M. Tymchenko, and A. Alù, Nonlinear metasurfaces: A paradigm shift in nonlinear optics, Mater. Today **21**, 8 (2018).
[10] C. Macklin, K. O'Brien, D. Hover, M. E. Schwartz, V. Bolkhovsky, X. Zhang, W. D. Oliver, and I. Siddiqi, A near quantum-limited Josephson traveling-wave parametric amplifier, Science **350**, 307 (2015).
[11] T. C. White, J. Y. Mutus, I. C. Hoi, R. Barends, B. Campbell, Y. Chen, Z. Chen, B. Chiaro, A. Dunsworth, E. Jeffrey, J. Kelly, A. Megrant, C. Neill, P. J. O'Malley, P. Roushan, D. Sank, A. Vainsencher, J. Wenner, S. Chaudhuri, J. Gao, and J. M. Martinis, Traveling wave

parametric amplifier with Josephson junctions using minimal resonator phase matching, Appl. Phys. Lett. **106**, 242601 (2015).

[12] A. B. Zorin, M. Khabipov, J. Dietel, and R. Dolata, Traveling-wave parametric amplifier based on three-wave mixing in a Josephson metamaterial, in *Proceedings of the 2017 16th International Superconductive Electronics Conference (ISEC)* (Institute of Electrical and Electronics Engineers Inc., Piscataway, NJ, 2018), Vol. 2018, pp. 1–3.

[13] A. Miano and O. A. Mukhanov, Symmetric traveling wave parametric amplifier, IEEE Trans. Appl. Supercond. **29**, 1501706 (2019).

[14] L. Planat, A. Ranadive, R. Dassonneville, J. Puertas Martínez, S. Léger, C. Naud, O. Buisson, W. Hasch-Guichard, D. M. Basko, and N. Roch, Photonic-Crystal Josephson Traveling-Wave Parametric Amplifier, Phys. Rev. X **10**, 021021 (2020).

[15] A. Ranadive, M. Esposito, L. Planat, E. Bonet, C. Naud, O. Buisson, W. Guichard, and N. Roch, A reversed Kerr traveling wave parametric amplifier, Nat. Comm. **13**, 1737 (2022).

[16] A. L. Grimsmo and A. Blais, Squeezing and quantum state engineering with Josephson travelling wave amplifiers, npj Quantum Inf. **3**, 20 (2017).

[17] M. Esposito, A. Ranadive, L. Planat, and N. Roch, Perspective on traveling wave microwave parametric amplifiers, Appl. Phys. Lett. **119**, 120501 (2021).

[18] L. Fasolo, A. Greco, E. Enrico, F. Illuminati, R. L. Franco, D. Vitali, and P. Livreri, Josephson travelling wave parametric amplifiers as non-classical light source for microwave quantum illumination, arXiv:2106.00522.

[19] C. Eichler, D. Bozyigit, C. Lang, M. Baur, L. Steffen, J. M. Fink, S. Filipp, and A. Wallraff, Observation of Two-Mode Squeezing in the Microwave Frequency Domain, Phys. Rev. Lett. **107**, 113601 (2011).

[20] E. Flurin, N. Roch, F. Mallet, M. H. Devoret, and B. Huard, Generating Entangled Microwave Radiation Over Two Transmission Lines, Phys. Rev. Lett. **109**, 183901 (2012).

[21] B. H. E. Flurin, N. Roch, J. D. Pillet, F. Mallet, E. Flurin, N. Roch, J. D. Pillet, F. Mallet, and B. Huard, Superconducting Quantum Node for Entanglement and Storage of Microwave Radiation, Phys. Rev. Lett. **114**, 090503 (2015).

[22] E. P. Menzel, R. Di Candia, F. Deppe, P. Eder, L. Zhong, M. Ihmig, M. Haeberlein, A. Baust, E. Hoffmann, D. Ballester, K. Inomata, T. Yamamoto, Y. Nakamura, E. Solano, A. Marx, and R. Gross, Path Entanglement of Continuous-Variable Quantum Microwaves, Phys. Rev. Lett. **109**, 250502 (2012).

[23] H. S. Ku, W. F. Kindel, F. Mallet, S. Glancy, K. D. Irwin, G. C. Hilton, L. R. Vale, and K. W. Lehnert, Generating and verifying entangled itinerant microwave fields with efficient and independent measurements, Phys. Rev. A **91**, 042305 (2015).

[24] K. G. Fedorov, L. Zhong, S. Pogorzalek, P. Eder, M. Fischer, J. Goetz, E. Xie, F. Wulschner, K. Inomata, T. Yamamoto, Y. Nakamura, R. Di Candia, U. Las Heras, M. Sanz, E. Solano, E. P. Menzel, F. Deppe, A. Marx, and R. Gross, Displacement of Propagating Squeezed Microwave States, Phys. Rev. Lett. **117**, 020502 (2016).

[25] K. G. Fedorov, S. Pogorzalek, U. Las Heras, M. Sanz, P. Yard, P. Eder, M. Fischer, J. Goetz, E. Xie, K. Inomata, Y. Nakamura, R. Di Candia, E. Solano, A. Marx, F. Deppe, and R. Gross, Finite-time quantum entanglement in propagating squeezed microwaves, Sci. Rep. **8**, 1 (2018).

[26] M. Westig, B. Kubala, O. Parlavecchio, Y. Mukharsky, C. Altimiras, P. Joyez, D. Vion, P. Roche, D. Esteve, M. Hofheinz, M. Trif, P. Simon, J. Ankerhold, and F. Portier, Emission of Nonclassical Radiation by Inelastic Cooper Pair Tunneling, Phys. Rev. Lett. **119**, 137001 (2017).

[27] J. C. Forgues, C. Lupien, and B. Reulet, Experimental Violation of Bell-like Inequalities by Electronic Shot Noise, Phys. Rev. Lett. **114**, 130403 (2015).

[28] C. M. Wilson, G. Johansson, A. Pourkabirian, M. Simoen, J. R. Johansson, T. Duty, F. Nori, and P. Delsing, Observation of the dynamical Casimir effect in a superconducting circuit, Nature (London) **479**, 376 (2011).

[29] B. H. Schneider, A. Bengtsson, I. M. Svensson, T. Aref, G. Johansson, J. Bylander, and P. Delsing, Observation of Broadband Entanglement in Microwave Radiation from a Single Time-Varying Boundary Condition, Phys. Rev. Lett. **124**, 140503 (2020).

[30] G. Andersson, S. W. Jolin, M. Scigliuzzo, R. Borgani, M. O. Tholén, D. B. Haviland, and P. Delsing, Squeezing and multimode entanglement of surface acoustic wave phonons, PRX Quantum **3**, 010312 (2022).

[31] C. L. Degen, F. Reinhard, and P. Cappellaro, Quantum sensing, Rev. Mod. Phys. **89**, 035002 (2017).

[32] S. Danilin and M. Weides, Quantum sensing with superconducting circuits, arXiv:2103.11022.

[33] K. M. Backes *et al.*, A quantum enhanced search for dark matter axions, Nature (London) **590**, 238 (2021).

[34] K. G. Fedorov, M. Renger, S. Pogorzalek, R. Di Candia, Q. Chen, Y. Nojiri, K. Inomata, Y. Nakamura, M. Partanen, A. Marx, R. Gross, and F. Deppe, Experimental quantum teleportation of propagating microwaves, arXiv:2103.04155.

[35] S. L. Braunstein and P. van Loock, Quantum information with continuous variables, Rev. Mod. Phys. **77**, 513 (2005).

[36] C. Weedbrook, S. Pirandola, R. García-Patrón, N. J. Cerf, T. C. Ralph, J. H. Shapiro, and S. Lloyd, Gaussian quantum information, Rev. Mod. Phys. **84**, 621 (2012).

[37] T. Hillmann, F. Quijandriá, G. Johansson, A. Ferraro, S. Gasparinetti, and G. Ferrini, Universal Gate Set for Continuous-Variable Quantum Computation with Microwave Circuits, Phys. Rev. Lett. **125**, 160501 (2020).

[38] M. Houde, L. C. G. Govia, and A. A. Clerk, Loss Asymmetries in Quantum Traveling-Wave Parametric Amplifiers, Phys. Rev. Applied **12**, 034054 (2019).

[39] S. Zhao and S. Withington, Quantum analysis of second-order effects in superconducting travelling-wave parametric amplifiers, J. Phys. D **54**, 365303 (2021).

[40] S. Shu, N. Klimovich, B. H. Eom, A. D. Beyer, R. B. Thakur, H. G. Leduc, and P. K. Day, Nonlinearity and wide-band parametric amplification in a (Nb,Ti)N microstrip transmission line, Phys. Rev. Research **3**, 023184 (2021).

[41] K. O'Brien, C. Macklin, I. Siddiqi, and X. Zhang, Resonant Phase Matching of Josephson Junction Traveling Wave Parametric Amplifiers, Phys. Rev. Lett. **113**, 157001 (2014).

[42] K. Peng, M. Naghiloo, J. Wang, G. D. Cunningham, Y. Ye, and K. P. O'Brien, Near-ideal quantum efficiency with a Floquet mode traveling wave parametric amplfier, arXiv:2104.08269.
[43] L. Planat, E. Al-Tavil, J. Puertas Martínez, R. Dassonneville, F. Foroughi, S. Léger, K. Bharadwaj, J. Delaforce, V. Milchakov, C. Naud, O. Buisson, W. Hasch-Guichard, and N. Roch, Fabrication and Characterization of Aluminum SQUID Transmission Lines, Phys. Rev. Applied **12**, 064017 (2019).
[44] L. Planat, Resonant and traveling-wave parametric amplification near the quantum limit, Ph.D. thesis, University Grenoble Alpes, 2020.
[45] S. Olivares, Quantum optics in the phase space, Eur. Phys. J. Special Topics **203**, 3 (2012).
[46] G. Adesso and F. Illuminati, Gaussian measures of entanglement versus negativities: Ordering of two-mode Gaussian states, Phys. Rev. A **72**, 032334 (2005).
[47] N. E. Frattini, U. Vool, S. Shankar, A. Narla, K. M. Sliwa, and M. H. Devoret, 3-wave mixing Josephson dipole element, Appl. Phys. Lett. **110**, 222603 (2017).
[48] See Supplemental Material at http://link.aps.org/supplemental/10.1103/PhysRevLett.128.153603 for details on the experimental setup, models, and calibration procedures, which includes Refs. [49–52].
[49] C. Lang, Quantum Microwave Radiation and its Interference Characterized by Correlation Function Measurements in Circuit Quantum Electrodynamics, Ph.D. thesis, ETH Zurich, 2014.
[50] M. Malnou, M. Vissers, J. Wheeler, J. Aumentado, J. Hubmayr, J. Ullom, and J. Gao, Three-wave mixing kinetic inductance traveling-wave amplifier with near-quantum-limited noise performance, PRX Quantum **2**, 010302 (2021).
[51] Technical data sheet: C20-0R518 Directional Coupler (Stripline).
[52] Technical data sheet: Coaxial Subminiature Multiport Switches R591722600.
[53] L. Spietz, K. W. Lehnert, I. Siddiqi, and R. J. Schoelkopf, Primary electronic thermometry using the shot noise of a tunnel junction, Science **300**, 1929 (2003).
[54] L. Spietz, R. J. Schoelkopf, and P. Pari, Shot noise thermometry down to 10 mK, Appl. Phys. Lett. **89**, 183123 (2006).
[55] S. W. Chang, J. Aumentado, W. T. Wong, and J. C. Bardin, Noise measurement of cryogenic low noise amplifiers using a tunnel-junction shot-noise source, in *IEEE MTT-S International Microwave Symposium Digest* (IEEE, San Francisco, CA, 2016).
[56] P. Horodecki, Separability criterion and inseparable mixed states with positive partial transposition, Phys. Lett. A **232**, 333 (1997).
[57] S. Boutin, D. M. Toyli, A. V. Venkatramani, A. W. Eddins, I. Siddiqi, and A. Blais, Effect of Higher-Order Nonlinearities on Amplification and Squeezing in Josephson Parametric Amplifiers, Phys. Rev. Applied **8**, 054030 (2017).
[58] G. Giedke, M. M. Wolf, O. Krüger, R. F. Werner, and J. I. Cirac, Entanglement of Formation for Symmetric Gaussian States, Phys. Rev. Lett. **91**, 107901 (2003).
[59] 10.5281/zenodo.5217996.